Journal of Power Sources 214 (2012) 178–184

Contents lists available at SciVerse ScienceDirect

Journal of Power Sources

journal homepage: www.elsevier.com/locate/jpowsour

Suppression of aluminum current collector corrosion in ionic liquid containing electrolytes

Ruben-Simon Kühnel, Mechthild Lübke, Martin Winter, Stefano Passerini, Andrea Balducci*

University of Muenster, Institute of Physical Chemistry-MEET, Corrensstr. 28/30, 48149 Muenster, Germany

HIGHLIGHTS

- $PYR_{14}TFSI$ added to LiTFSI-based organic electrolytes strongly suppresses Al corrosion.
- $Al(TFSI)_3$, which plays a crucial role in the Al protection, was synthesized.
- Solubility tests with $Al(TFSI)_3$ confirmed its low solubility in $PYR_{14}TFSI$.

GRAPHICAL ABSTRACT

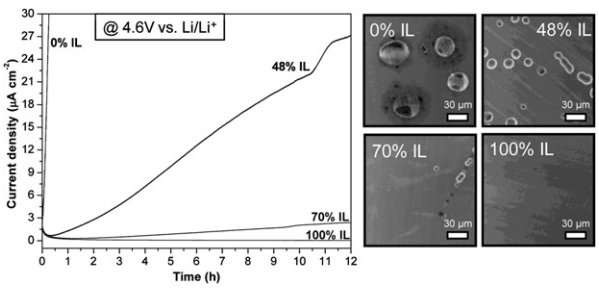

ARTICLE INFO

Article history:
Received 23 December 2011
Received in revised form
10 March 2012
Accepted 22 April 2012
Available online 8 May 2012

Keywords:
Aluminum corrosion suppression
Ionic liquid
PC
Mixtures
$Al(TFSI)_3$ solubility

ABSTRACT

Solutions of LiTFSI in organic solvents such as carbonates, do not display the ability to prevent the aluminum corrosion and for this reason cannot be conveniently used as electrolytes in LIBs. However, addition of $PYR_{14}TFSI$ to PC–LiTFSI strongly suppresses the aluminum corrosion process, both at 20 °C and 60 °C. At 60 °C, in a mixture PC–$PYR_{14}TFSI$–LiTFSI containing 50% of IL, the charge involved in the corrosion process is one order of magnitude lower than that observed in PC–LiTFSI. The suppression of the corrosion process by $PYR_{14}TFSI$ might be related to the reduced solubility of $Al(TFSI)_3$ in $PYR_{14}TFSI$ compared to PC. $Al(TFSI)_3$ is formed on the Al surface in electrolytes containing LiTFSI, and the low solubility of this compound in $PYR_{14}TFSI$ contributes to the formation of a stable protective layer on the Al surface, which in turn reduces the corrosion process. Thanks to their ability to suppress the Al corrosion, PC–$PYR_{14}TFSI$–LiTFSI mixtures can be conveniently used as electrolytes in LIBs, both at room temperature and 60 °C.

1. Introduction

Lithium-ion batteries (LIBs) are nowadays considered one of the most important energy storage devices. LIBs are currently dominating the consumer electronic market and they have been indicated as the most promising option for the next generation of hybrid and electric vehicles (HVs and EVs). Moreover, they are also considered as an attractive candidate for the realization of high-efficiency delocalized energy storage [1].

The electrolytes presently used in commercial LIBs are based on mixtures of organic carbonates and contain lithium hexafluorophosphate ($LiPF_6$) as lithium salt [1,2]. The use of these electrolytes allows high performance in terms of energy and cycle life. However, since these electrolytes are flammable and volatile, their use poses serious safety risks and strongly reduces the temperature range of use. Hence, in order to introduce LIBs in new applications, particularly in HVs and EVs, advanced electrolytes with improved safety and the ability to work in a broader operative temperature range are urgently needed. Clearly, in order to be

* Corresponding author. Tel.: +49 2518336083; fax: +49 2518336084.
E-mail address: andrea.balducci@uni-muenster.de (A. Balducci).

0378-7753/$ – see front matter © 2012 Elsevier B.V. All rights reserved.
doi:10.1016/j.jpowsour.2012.04.054

really effective, the introduction of such advanced electrolytes cannot lead to a reduction of the overall performance.

In the last years, the use of ionic liquids (ILs) as electrolytes for LIBs has been intensively investigated. The main advantages of ILs with respect to organic carbonates are their non-flammability, negligible vapor pressure and high chemical and thermal stability [3,4]. Moreover, some ILs display good conductivity and large electrochemical stability window (ESW). The results of these studies showed that ILs positively contribute to the safety of batteries and indicate these electrolytes as one of the most attractive candidates for the replacement of organic electrolytes [5]. However, when the performance of IL-based systems is compared with that of LIBs containing conventional electrolytes further improvement appears necessary, especially during testing at high current rate [5].

With the aim to combine the favorable properties of conventional electrolytes and ILs, the use of electrolytic solutions containing mixtures of these two electrolytes has been investigated. Recent works showed that the use of such mixtures is a promising strategy for the realization of advanced electrolytes for LIBs, with properties that can be advantageously tailored varying the amount of IL inside the mixtures [6–11]. Among the mixtures investigated so far, those containing propylene carbonate (PC), the ionic liquid *N*-butyl-*N*-methylpyrrolidinium bis(trifluoromethanesulfonyl) imide ($PYR_{14}TFSI$) and lithium bis(trifluoromethanesulfonyl)imide (LiTFSI) appear of particular interest. As a matter of fact, depending on their composition, such mixtures can display high conductivity, a flash point much higher than those of conventional organic electrolytes and they can also be non-flammable [11]. Moreover, they contain LiTFSI as lithium salt.

As mentioned earlier, $LiPF_6$ is currently used as lithium salt in commercial LIBs. $LiPF_6$ displays a favorable combination of properties and allows the realization of electrolytes with high conductivity and good electrochemical stability. Moreover, the use of $LiPF_6$ also guarantees an excellent protection of the aluminum current collector used for the cathode of LIBs. Unfortunately, $LiPF_6$ shows a relatively low thermal and chemical stability and it is extremely sensitive to water, which might be present in LIB electrolytes. The presence of water traces leads to HF formation in the electrolytic solution, which in turn causes decomposition of the electrolyte solvent. HF can also attack some active materials, *e.g.* dissolute Mn^{2+} species of $LiMn_2O_4$ spinel based cathode materials [2]. For that, electrolytes containing $LiPF_6$ and organic carbonates suffer from an intrinsic chemical instability, which becomes more severe at temperatures above 60 °C [2].

Since several years, LiTFSI has been indicated as a possible replacement for $LiPF_6$. LiTFSI can be used for the realization of electrolytes with high conductivity and high electrochemical stability. In addition, it displays better thermal and chemical stabilities, *e.g.* no moisture sensitivity, compared to $LiPF_6$. Consequently, the introduction of this salt in LIBs could positively contribute to the safety as well as to the widening of the temperature range of use of these devices [2]. However, LiTFSI does not guarantee an adequate aluminum corrosion protection when used in combination with organic carbonates like PC [12].

In 2004 Garcia *et al.* reported that in ionic liquids containing TFSI as anion, the aluminum corrosion is effectively suppressed without the need of a Li salt that is known to form a protective layer in organic carbonates [13]. Considering these results, the use of LiTFSI seems therefore to be possible in IL-based electrolytes. Interestingly, the results obtained with the PC–$PYR_{14}TFSI$–LiTFSI mixtures indicated that in these electrolytes the potential at which the aluminum corrosion becomes significant strongly depends on the amount of $PYR_{14}TFSI$. In mixtures containing high amounts of $PYR_{14}TFSI$, the aluminum corrosion process is shifted toward potentials significantly higher than those of mixtures containing low amounts of $PYR_{14}TFSI$ [11]. For that, it is reasonable to suppose that TFSI-based ionic liquids might have the ability to suppress the aluminum corrosion process also when mixed with organic carbonates and LiTFSI. This effect could be extremely interesting in view of the use of LiTFSI in LIBs. Nevertheless, only few works investigated in detail the influence of ILs on the aluminum corrosion process of electrolyte containing LiTFSI.

This manuscript reports about the influence of $PYR_{14}TFSI$ on the aluminum corrosion properties of PC–$PYR_{14}TFSI$–LiTFSI mixtures. The Al corrosion properties were investigated by means of chronoamperometry, cyclic voltammetry (CV), scanning electron microscopy (SEM), X-ray photoelectron spectroscopy (XPS) and $Al(TFSI)_3$ solubility experiments. Furthermore, the influence of the corrosion process on the electrochemical performance of lithium iron phosphate ($LiFePO_4$, LFP) electrodes was considered.

2. Experimental

2.1. Electrolyte preparation

Propylene carbonate (UBE, Japan) was used as received. $PYR_{14}TFSI$ was synthesized as reported earlier [11]. Several electrolytes based on mixtures of PC and $PYR_{14}TFSI$ and two electrolytes containing only the single components were prepared. LiTFSI (3M battery grade) was used as Li-salt. The concentration of LiTFSI was fixed to 0.3 mol dm^{-3} for all the electrolytes. The water content of all prepared electrolytes was less than 10 ppm, as verified by Karl Fischer titration. In the following, electrolyte compositions are always defined with respect to the mole percentage of the solvent components.

2.2. Electrochemical and morphological characterization

Anodic aluminum corrosion tests were carried out using a three-electrode Swagelok cell connected to a Solartron model 1287A potentiostat controlled by Corrware software. As working electrode, discs of 12 mm diameter cut out of aluminum foil (99.95%, thickness of 30 μm, rinsed with ethanol, then vacuum dried) were used. Lithium was used as both counter and reference electrodes. The chronoamperometry experiments were carried out at room temperature and the cyclic voltammetry experiments were carried out at 20 and 60 °C using a Binder MK53 climatic chamber.

Chronoamperometry. Initially, the potential of the working electrode was linearly swept from open circuit potential (OCP) to 4.6 V vs. Li/Li^+ at a sweep rate of 1 mV s^{-1}. The potential was then hold for 12 h at 4.6 V vs. Li/Li^+ and the current was continuously recorded.

Cyclic voltammetry. Starting from OCP, the potential was scanned to 5.4 V vs. Li/Li^+, the scanning direction was reversed and the potential was scanned down to 3.3 V vs. Li/Li^+. The scan rate was fixed to 5 mV s^{-1}. A total of 10 cycles were performed for each cell.

The morphology of Al foil electrodes that had been polarized for 12 h at a potential of 4.6 V was investigated (after rinsing with dimethyl carbonate (DMC) and drying under vacuum) by scanning electron microscopy (AURIGA, Carl Zeiss).

2.3. Surface characterization

The surface of the aluminum foils subjected to polarization for 12 h at 4.6 V vs. Li/Li^+ was characterized by means of XPS. The Al foils were rinsed with diethyl carbonate and dried under vacuum. The XPS measurements were performed on an Axis ultra DLD (Kratos) using monochromatic Al Kα radiation at 1486.7 eV. The irradiated area on the sample surface was about 300 μm × 700 μm. The measurements were repeated at three different points. The core scans were

performed at pass energies of 20 eV. The calibration of the spectra was done with respect to adventitious carbon (284 eV). The samples were transferred from the drybox into the vacuum chamber without any air contact by using an argon filled transfer box.

2.4. Synthesis and solubility tests of $Al(TFSI)_3$

$Al(TFSI)_3$ was synthesized based on a procedure described in reference [14]. 2 g of H-TFSI (99%, Acros Organics) were dissolved in 9 cm^3 of purified H_2O. Then, 0.3 g of Al pieces cut out of an Al foil (99.95%, thickness of 30 μm, rinsed with ethanol, then vacuum dried) were added to the solution, which was heated under reflux for 8 h. After filtering off the residual Al, the remaining solution was concentrated using a rotary evaporator, and then pre-dried at 80 °C under *ca.* 20 mbar of pressure. Drying at up to 140 °C and *ca.* 0.01 mbar resulted in a white powder. The composition was verified by mass spectroscopy and nuclear magnetic resonance spectroscopy (NMR).

In order to investigate the solubility kinetics of $Al(TFSI)_3$ in the investigated electrolytes, conductivity experiments were carried out. The change in relative electrolyte resistance (relative to the resistance of the pure electrolyte without any addition of $Al(TFSI)_3$) due to the dissolution of $Al(TFSI)_3$ in the electrolyte was measured. For that, 20 mg of $Al(TFSI)_3$ were added to 0.7 ml of electrolyte, and the change in electrolyte resistance was recorded for 15 h by impedance spectroscopy. As setup, we used a two-electrode conductivity cell (both electrodes were made of platinum) connected to a Solartron model 1287A potentiostat and a Solartron model SI 1260 impedance/gain-phase analyzer controlled by Corrware and ZPlot software (Scribner Associates). The frequency was scanned from 1 MHz to 10 Hz, while the amplitude was set to 5 mHz. Electrolyte resistances were then calculated from the intercept of the complex impedance curve with the real axis in the Nyquist plot. To evaluate the rate of $Al(TFSI)_3$ dissolution, we also measured the resistance of the considered electrolyte solutions with 7 mg $Al(TFSI)_3$ already dissolved in 0.7 mL of electrolytes. The $Al(TFSI)_3$ solubility experiments were carried out in a BINDER MK53 climatic chamber at 40 °C.

2.5. LFP electrode preparation and constant current cycling

Carbon-coated $LiFePO_4$ was obtained by a commercial supplier (Süd-Chemie, Germany) and used as received. Sodium carboxymethyl cellulose (CMC) was provided by Dow Wolff Cellulosics (Walocel CRT 2000 PPA 12) with a degree of substitution of 1.2. Carbon black (Super-P, TIMCAL) was used as conducting agent. Composite electrodes coated on Al foil were prepared following a procedure described in reference [11]. The composition of the dried electrodes was 85 wt% $LiFePO_4$, 10 wt% Super-P and 5 wt% of CMC. The electrode mass loading was *ca.* 1.5 mg cm^{-2}. The electrode area was 1.12 cm^2.

Constant current cycling tests were carried out in three-electrode Swagelok cells. The cells were assembled in a glove box (MBRAUN). Metallic lithium (Chemetall) was used for the counter and reference electrodes. As separator, a stack of Freudenberg fleeces (FS2190) drenched with 80 mm^3 of electrolyte was used. The cycling experiments were carried out between 2.8 and 4.2 V vs. Li/Li^+ using a MACCOR Series 4000 battery tester at 60 °C. Initially, 50 cycles at 1 C were carried out. After that, a loop of 5 cycles at C/5 and 5 cycles at 3 C was repeated for 9 times.

3. Results and discussion

It is known that when LiTFSI is used in combination with organic carbonate, *e.g.* PC, severe corrosion of Al current collectors occurs [12]. However, some reports indicated that when this salt is used in combination with TFSI-based ILs, the Al corrosion is strongly suppressed [13,15–17]. Fig. 1 shows the results obtained during a chronoamperometric experiment in which Al foils were hold for 12 h at 4.6 V vs. Li/Li^+ in PC–LiTFSI, $PYR_{14}TFSI$–LiTFSI and PC–$PYR_{14}TFSI$–LiTFSI mixtures, at room temperature. As shown, the current density recorded during the experiments, which can be associated to the corrosion process occurring on the surface of the Al foil, strongly depended on the electrolyte composition. In PC–LiTFSI the current density increased over time and after 2 h reached a value exceeding 230 μA cm^{-2} (Fig. 1a), confirming the occurrence of a corrosion process in this electrolyte. To the contrary, in $PYR_{14}TFSI$–LiTFSI the current density decreased continuously and after 12 h reached a value lower than 1 μA cm^{-2}, confirming the excellent aluminum corrosion protection in this IL (Fig. 1a,b). Interestingly, in the PC–$PYR_{14}TFSI$–LiTFSI mixtures the detected current densities were significantly smaller than that in PC–LiTFSI, but rather similar to that of $PYR_{14}TFSI$–LiTFSI (Fig. 1a). As shown in Fig. 1b, the higher was the $PYR_{14}TFSI$ content, the smaller was the slope of the corrosion current curve. For example, an Al foil polarized in a mixed solution of 30% PC, 70% $PYR_{14}TFSI$ and LiTFSI displayed a current density of *ca.* 2.5 μA cm^{-2} after 12 h. This value was higher than that observed in $PYR_{14}TFSI$–LiTFSI, but it was almost two orders of magnitude lower than that in PC–LiTFSI.

The results of these tests clearly indicated that the addition of $PYR_{14}TFSI$ to PC–LiTFSI strongly reduces the corrosion current. The suppression of the corrosion process caused by the presence of $PYR_{14}TFSI$ was also well visible on the SEM images of the polarized Al foils. As shown in Fig. 2, the foil polarized in PC–LiTFSI showed

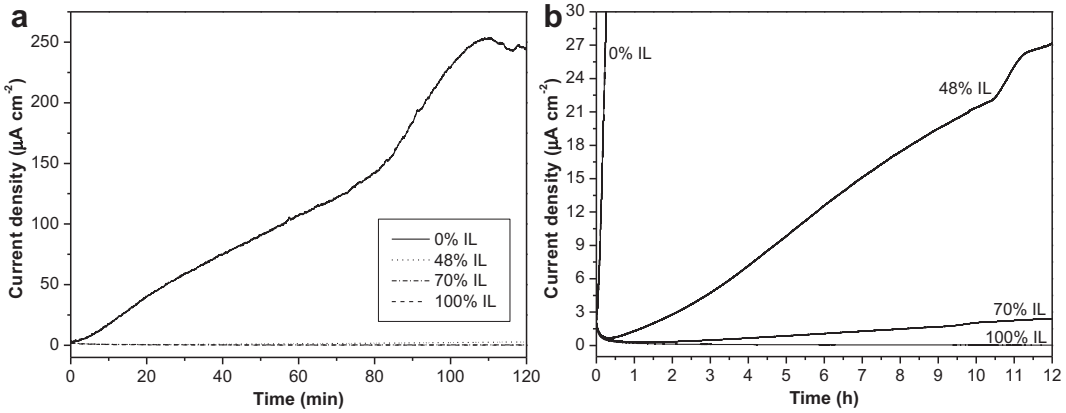

Fig. 1. a) Chronoamperograms of Al electrodes recorded during prolonged charging at 4.6 V vs. Li/Li^+ in PC–LiTFSI, $PYR_{14}TFSI$–LiTFSI and in PC–$PYR_{14}TFSI$–LiTFSI mixtures at room temperature. Li was used for the counter and reference electrodes. b) Magnification.

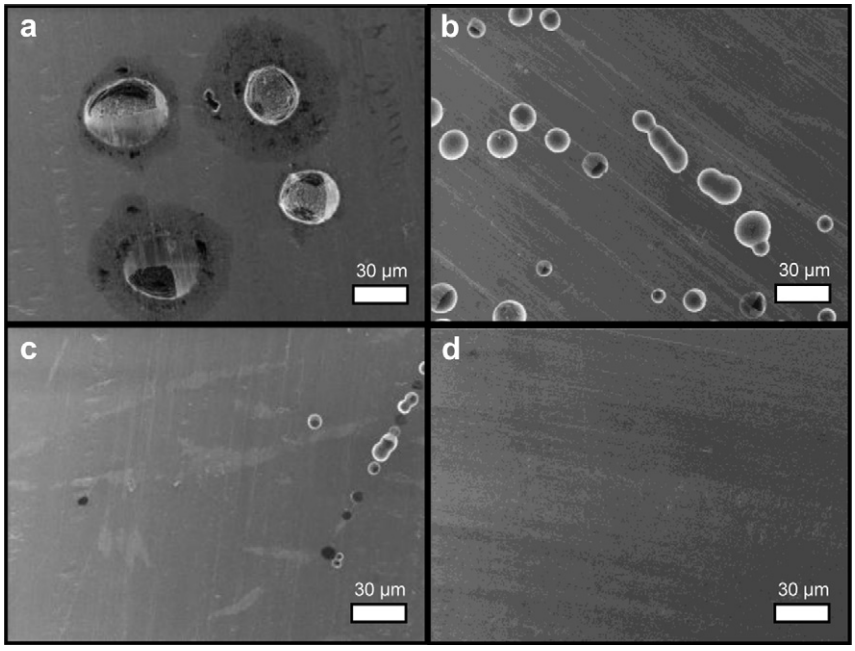

Fig. 2. SEM images of Al electrodes polarized for 12 h at 4.6 V vs. Li/Li+ at room temperature in PC–0.3 M LiTFSI (a), PC–PYR14TFSI–0.3 M LiTFSI (IL content 48 mol% (b); IL content 70 mol% (c)) and PYR14TFSI–0.3 M LiTFSI (d).

seriously corroded areas (Fig. 2a). Some of the corrosion pits went through the whole thickness of the foil. Also, the surroundings of the pits showed signs of corrosion. This behavior is typical for Al foils subject to a corrosion process in TFSI-based organic electrolytes [12,18]. The addition of $PYR_{14}TFSI$ significantly changed the number, the shape and the size of the pits. As shown in Fig. 2b and c, the number of pits formed on the Al surface significantly decreased by the addition of $PYR_{14}TFSI$. Moreover, the higher was the $PYR_{14}TFSI$ content of the electrolyte, the smaller and more superficial (not reaching deep into the Al) were the pits on the Al surface. The Al foil polarized in $PYR_{14}TFSI$–LiTFSI showed no sign of corrosion in good agreement with the very low current density recorded in the chronoamperometric experiment (Fig. 2d).

In order to further investigate the influence of the $PYR_{14}TFSI$ content on the Al corrosion, 10 consecutive CVs were than conducted between 3.3 and 5.4 V vs. Li/Li^+, at 20 and 60 °C. Fig. 3 shows the cumulative charge calculated from the CVs in the investigated electrolytes. As shown in the figure, at 20 °C the charge in PC–LiTFSI was more than one order of magnitude higher compared to $PYR_{14}TFSI$–LiTFSI. The charge calculated for a mixture containing only 19% of $PYR_{14}TFSI$ was about one quarter that of PC–LiTFSI, thus indicating that the addition of $PYR_{14}TFSI$ dramatically reduces the charge involved in the Al corrosion process. When 48% of $PYR_{14}TFSI$ was present in the mixture, the charge was almost comparable to that of the pure IL. At 60 °C, the suppression of the corrosion process by $PYR_{14}TFSI$ was even more marked. As shown in the figure, at this temperature the presence of 48% of $PYR_{14}TFSI$ in the mixture reduced the charge involved in the corrosion of more than one order of magnitude compared to PC–LiTFSI. It is interesting to note that starting from this amount of IL inside the mixture, the charge involved in the corrosion process became comparable with that observed at 20 °C, indicating that the suppression of the corrosion is significant also at high temperature.

Considering the results so far available, the reason why LiTFSI does not guarantee adequate aluminum corrosion protection when used in combination with PC and other organic carbonates appears to be related to the mechanism of Al oxidative dissolution [12]. Wang *et al.* [19] proposed a mechanism of Al dissolution in LiTFSI-based electrolytes involving the formation on the Al foil surface of Al-TFSI complexes, which dissolve and diffuse into the electrolyte. The importance of the solubility of such Al-TFSI complexes in the electrolyte solution was clearly evidenced. If these complexes are easily soluble in the electrolyte solution, Al corrosion should be severe, whereas Al corrosion should be suppressed if the Al-TFSI complexes are hardly soluble in the electrolyte. Garcia *et al.* [13] were the first to report the suppression of Al corrosion in LiTFSI-based ionic liquid electrolyte. They also proposed the formation of an Al-TFSI complex insoluble in ionic liquids, which is thus protecting the Al surface.

Peng *et al.* [20] polarized Al foils in LiTFSI/1-butyl-3-methylimidazolium-TFSI and analyzed the surface film formed on the Al

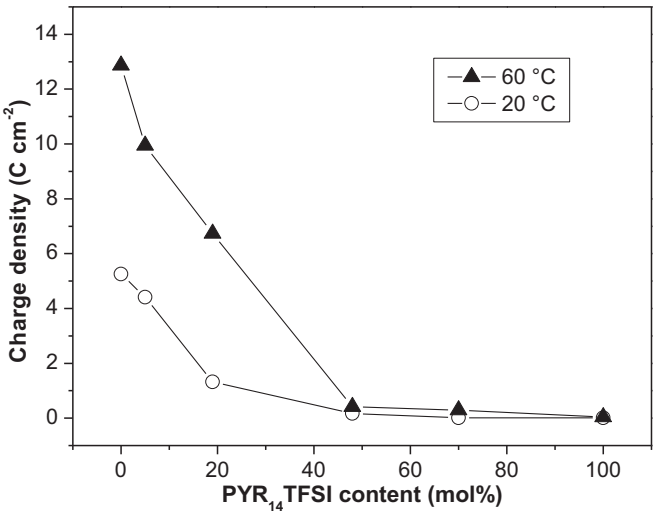

Fig. 3. Accumulated specific charges calculated by integrating the anodic currents over 10 cycles of cyclic voltammetry of Al electrodes in PC–0.3 M LiTFSI, PC–$PYR_{14}TFSI$–0.3 M LiTFSI (with a variable content of $PYR_{14}TFSI$) and $PYR_{14}TFSI$–0.3 M LiTFSI. Li was used for the counter and reference electrodes. The electrodes were cycled at 20 and 60 °C with a scan rate of 5 mV s^1 between 3.3 and 5.4 V vs. Li/Li^+.

by means of X-ray photoelectron spectroscopy. They found the protective layer on the Al to be composed on the outside of Al-TFSI species and in the inside of Al_2O_3 and AlF_3. They proposed that the AlF_3 is a decomposition product of Al-TFSI species. Putting all these findings together, it seems very likely that the mechanism of Al corrosion in electrolytes containing the TFSI anion involves the formation of Al-TFSI species on the surface of the Al foil. Particularly, the solubility of Al-TFSI in the electrolyte solution appears to be of great importance since it could be one of the reasons for the different behavior of the electrolytes considered above.

Therefore we also investigated the chemical nature of the surface films formed on the investigated Al foil by means of XPS. Fig. 4 a shows the spectra of Al, O and C as obtained on the unpolarized Al foil. In this foil, the air-formed oxide layer had a typical thickness of 2.5 nm as estimated from the XPS measurements (Fig. 4). After polarizing such an Al foil for 12 h at 4.6 V vs. Li/Li^+ the composition of the surface layer changed and new peaks for C, O, F, N and S appeared (Fig. 4b). These peaks correspond to those found by Peng *et al.* [20] and Howlett *et al.* [21] for TFSI and pyrrolidinium species. The presence of the N-peak at higher binding energy (from pyrrolidinium species) indicates residual ionic liquid. To rule out that the XPS signals are solely due to residual electrolyte we compared the ratios between TFSI and PYR_{14} ions in the considered electrolytes with the ratios between the areal intensities of the N-peaks corresponding to the TFSI and PYR_{14} ions (Table 1). The excess of TFSI found on the Al surface as compared to the prediction from the composition of the electrolytes points toward the presence of other TFSI species. Furthermore, the amount of excess TFSI seems to increase with the PC content of the electrolyte. Considering the above mentioned Al corrosion mechanism for LiTFSI-based electrolytes and the spectroscopic findings, the formation of $Al(TFSI)_3$ during polarization of Al foils in LiTFSI-based electrolytes seems therefore reasonable. However, it cannot be completely excluded the hypothesis that the excess TFSI was (also) partly due to crystallized LiTFSI.

Table 1
a) Calculated molar fractions of TFSI and PYR_{14} units with respect to the amount of N-containing species in different PC–PYR_{14}TFSI–0.3 M LiTFSI electrolytes. b) Estimated molar fractions (from N-peaks in XPS spectra) of TFSI and PYR_{14} units with respect to the amount of N-containing species on the surface of Al foil electrodes polarized at 4.6 V vs. Li/Li^+ for 12 h.

Electrolyte		A) in the electrolyte (calculated)		B) on the Al surface (estimated from XPS meas.)	
mol% PC	mol% IL	w(PYR_{14}) /%	w(TFSI) /%	w(PYR_{14}) /%	w(TFSI) /%
52	48	47.1	52.9	26.6	73.4
30	70	47.5	52.5	44.0	56.0
0	100	47.7	52.3	43.2	56.8

Assuming that the formation of $Al(TFSI)_3$ takes place as essential step of the corrosion process, the corrosion rate should be higher in those electrolytes that readily dissolve $Al(TFSI)_3$, whereas electrolytes with a very low solubility of $Al(TFSI)_3$ might inhibit Al corrosion because the formed $Al(TFSI)_3$ would act as a passivation layer. With the aim to understand this important point, we therefore synthesized $Al(TFSI)_3$ and investigated its solubility in PC–LiTFSI, PYR_{14}TFSI–LiTFSI and PC–PYR_{14}TFSI–LiTFSI mixtures. Fig. 5 shows the change in relative electrolyte resistance over 15 h after the addition of 20 mg of $Al(TFSI)_3$ to 0.7 ml of electrolyte. A change in the electrolyte resistance clearly indicates dissolution of $Al(TFSI)_3$. As shown in the figure, after 15 h, the resistance of PC–LiTFSI changed, indicating that $Al(TFSI)_3$ is soluble in this electrolyte. After this time,

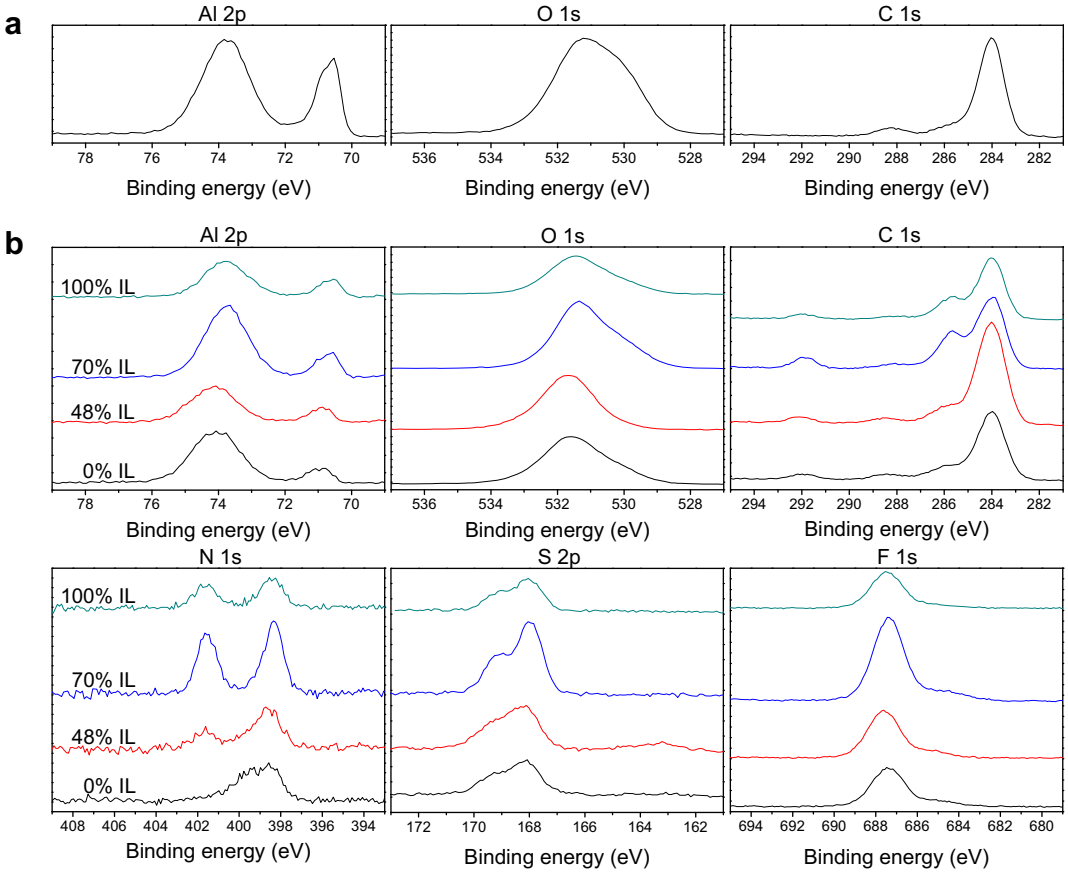

Fig. 4. a) Al 2p, O 1s and C 1s XPS spectra of an unpolarized Al foil. b) Al 2p, N 1s, S 2p, O 1s, C 1s and F 1s XPS spectra (normalized intensities) of Al electrodes polarized at 4.6 V vs. Li/Li^+ for 12 h at room temperature in PC–0.3 M LiTFSI, PC–PYR_{14}TFSI–0.3 M LiTFSI (IL content 48 mol%; IL content 70 mol%) and PYR_{14}TFSI–0.3 M LiTFSI (from bottom to top).

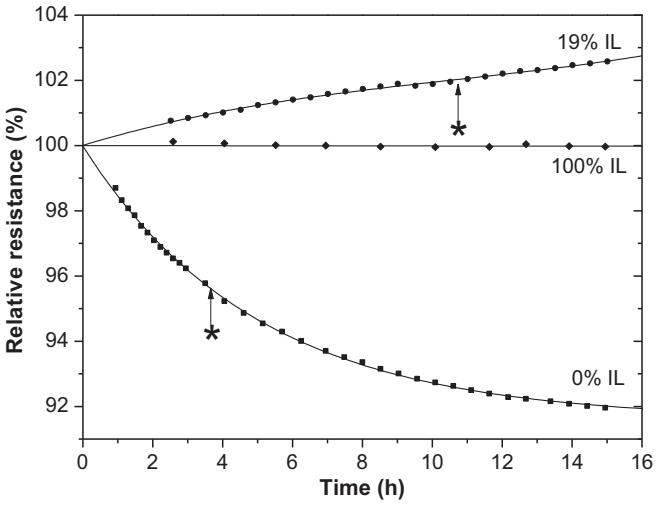

Fig. 5. $Al(TFSI)_3$ solubility test in PC–0.3 M LiTFSI, PC–$PYR_{14}TFSI$–0.3 M LiTFSI (containing 19% $PYR_{14}TFSI$) and $PYR_{14}TFSI$–0.3 M LiTFSI. 20 mg of $Al(TFSI)_3$ were added to 0.7 ml electrolyte solution. Afterward, the change in electrolyte resistance was recorded over *ca.* 15 h using a two-electrode conductivity cell (both electrodes were made of platinum). The experiment was conducted at 40 °C.

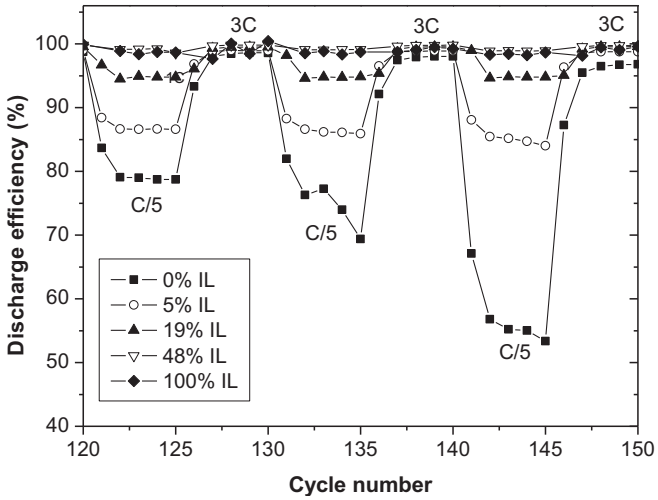

Fig. 6. Coulombic efficiency calculated during the charge–discharge process of LFP electrodes in PC–0.3 M LiTFSI, PC–$PYR_{14}TFSI$–0.3 M LiTFSI (with a variable content of $PYR_{14}TFSI$) and $PYR_{14}TFSI$–0.3 M LiTFSI between 2.8 and 4.2 V vs. Li/Li^+. Li was used for the counter and reference electrodes. The electrodes were cycled at 60 °C.

the resistance reached an almost steady state value, indicating that almost all of the $Al(TFSI)_3$ was dissolved. In contrast, the dissolution of $Al(TFSI)_3$ was practically absent in $PYR_{14}TFSI$–LiTFSI since after 15 h the electrolyte resistance did not change. In the case of a mixture PC–$PYR_{14}TFSI$–LiTFSI containing 19 mol% of IL the relative resistance increased over time, but also did not reach a plateau value. The increase of resistance can be explained considering that the number of ions in this electrolyte solution was already quite high before the dissolution of $Al(TFSI)_3$. Thus, the dominant factor of additional ions is increased ion–ion interactions leading to a higher solution resistance. In order to better understand the different solubility of $Al(TFSI)_3$, the time of dissolution of a defined amount of salt in the considered electrolytes was also investigated. For that, 7 mg of $Al(TFSI)_3$ were introduced in the electrolytes at 40 °C. The dissolution of these 7 mg took three times longer in the mixture with 19% of IL than in the pure PC electrolyte (see Fig. 5). Considering these results, the reduced solubility of $Al(TFSI)_3$ in PC–LiTFSI by the addition of $PYR_{14}TFSI$ appears to be a very reasonable explanation for the suppressed Al corrosion in the PC–$PYR_{14}TFSI$–LiTFSI mixtures. However, further investigations are still needed to prove the proposed Al corrosion mechanism in LiTFSI-based electrolytes.

With the aim to investigate the influence of the Al corrosion on the performance of LIB electrodes, we finally investigated the coulombic efficiency of the charge–discharge process of LFP electrodes used in combination with the electrolytes considered above, at 60 °C. During these tests, the LFP electrodes were cycled between 2.8 and 4.2 V vs. Li/Li^+. Since the Al corrosion was reported to take place at above 3.55 V vs. Li/Li^+ in LiTFSI-based electrolytes, the LFP electrodes were operated in a potential region in which the Al corrosion process was likely to occur. Hence, the coulombic efficiency of the charge–discharge process of the LFP electrodes should change depending on the ability of the used electrolyte to suppress the Al corrosion. Initially the electrodes were subjected to 50 cycles at 1C. After that, a loop of 5 cycles at C/5 and 5 cycles at 3 C was repeated for 9 times. This protocol was selected because the Al corrosion might be more pronounced during slow cycling because of the longer permanence at high potential. The high current, in fact, might drive the potential up to quickly to the cut-off potential, thus reducing the time for the corrosion process to occur. As shown in Fig. 6, during cycles carried out at 3 C, the efficiencies of the LFP electrodes were generally close to 100%, independent of the used electrolyte. However, during cycles carried out at C/5 the cycling efficiencies of the electrodes were strongly influenced by the electrolyte composition, and the higher was the $PYR_{14}TFSI$ content, the higher was the efficiency during cycling. For example, the efficiency of the charge–discharge process in PC–LiTFSI at the end of the test was only 50%. The presence of 5% of $PYR_{14}TFSI$ in the electrolyte improved the efficiency to 80%. In electrolytes containing 50% or more of $PYR_{14}TFSI$ the LFP electrodes displayed efficiencies close to 100% during all tests.

4. Conclusions

The use of mixtures of ionic liquids and organic carbonates is a convenient strategy for the realization of advanced electrolytes for LIBs, particularly because the properties of these electrolytes can be advantageously tailored varying the amount of IL. The results of this study clearly indicate that the addition of appropriate amounts of $PYR_{14}TFSI$ to PC–LiTFSI electrolytes has the ability to suppress Al corrosion. This is especially important because it allows the use of the LiTFSI salt, which is superior to $LiPF_6$ both in terms of chemical and thermal stability.

Furthermore, we demonstrated for the first time that the compound $Al(TFSI)_3$, which might play a crucial role in protecting Al corrosion in PC–$PYR_{14}TFSI$–LiTFSI mixtures, is indeed hardly soluble in $PYR_{14}TFSI$.

Acknowledgments

The authors wish to thank Sebastian Menne for taking the SEM images, Uta Rodehorst for the XPS measurements and the Westfälische Wilhelms-Universität Münster and the Ministerium für Innovation, Wissenschaft, Forschung und Technologie des Landes Nordrhein-Westfalen (MIWFT) for the financial support. We gratefully appreciated the supply of materials by Süd-Chemie AG ($LiFePO_4$).

References

[1] B. Scrosati, J. Garche, J. Power Sources 195 (2010) 2419.
[2] K. Xu, Chem. Rev. 104 (2004) 4303.
[3] M. Galiński, A. Lewandowski, I. Stępniak, Electrochim. Acta 51 (2006) 5567.
[4] M. Armand, F. Endres, D.R. MacFarlane, H. Ohno, B. Scrosati, Nat. Mater. 8 (2009) 621.

[5] A. Balducci, S.S. Jeong, G.T. Kim, S. Passerini, M. Winter, M. Schmuck, G.B. Appetecchi, R. Marcilla, D. Mecerreyes, V. Barsukov, V. Khomenko, I. Cantero, I. De Meatza, M. Holzapfel, N. Tran, J. Power Sources 196 (2011) 9719.
[6] A. Chagnes, M. Diaw, B. Carré, P. Willmann, D. Lemordant, J. Power Sources 145 (2005) 82.
[7] J.-A. Choi, E.-G. Shim, B. Scrosati, D.-W. Kim, Bull. Korean Chem. Soc. 31 (2010) 3190.
[8] H.F. Xiang, B. Yin, H. Wang, H.W. Lin, X.W. Ge, S. Xie, C.H. Chen, Electrochim. Acta 55 (2010) 5204.
[9] G.H. Lane, A.S. Best, D.R. MacFarlane, M. Forsyth, P.M. Bayley, A.F. Hollenkamp, Electrochim. Acta 55 (2010) 8947.
[10] A. Guerfi, M. Dontigny, M. Petitclerc, M. Lagacé, A. Vijh, K. Zaghib, J. Power Sources 195 (2010) 845.
[11] R.-S. Kühnel, N. Böckenfeld, S. Passerini, M. Winter, A. Balducci, Electrochim. Acta 56 (2011) 4092.
[12] S.-T. Myung, Y. Hitoshi, Y.-K. Sun, J. Mater. Chem. 21 (2011) 9891.
[13] B. Garcia, M. Armand, J. Power Sources 132 (2004) 206.
[14] M.J. Earle, B.J. Mcauley, A. Ramani, K.R. Seddon, J.M. Thomson, United States Patent US6998497 (2006).
[15] C. Peng, L. Yang, Z. Zhang, K. Tachibana, Y. Yang, J. Power Sources 173 (2007) 510.
[16] M. Nadherna, R. Dominko, D. Hanzel, J. Reiter, M. Gaberscek, J. Electrochem. Soc. 156 (2009) A619.
[17] J. Mun, T. Yim, C.Y. Choi, J.H. Ryu, Y.G. Kim, S.M. Oh, Electrochem. Solid-State Lett. 13 (2010) A109.
[18] S.-W. Song, T.J. Richardson, G.V. Zhuang, T.M. Devine, J.W. Evans, Electrochim. Acta 49 (2004) 1483.
[19] X. Wang, E. Yasukawa, S. Mori, Electrochim. Acta 45 (2000) 2677.
[20] C. Peng, L. Yang, Z. Zhang, K. Tachibana, Y. Yang, S. Zhao, Electrochim. Acta 53 (2008) 4764.
[21] P.C. Howlett, N. Brack, A.F. Hollenkamp, M. Forsyth, D.R. MacFarlane, J. Electrochem. Soc. 153 (2006) A595.